HHS Public Access

Author manuscript

J Surg Res. Author manuscript; available in PMC 2024 April 30.

Published in final edited form as:

J Surg Res. 2024 January ; 293: 701–708. doi:10.1016/j.jss.2023.08.038.

Humanized Anti-Carcinoembryonic Antigen Antibodies Brightly Target and Label Gastric Cancer in Orthotopic Mouse Models

Kristin E. Cox, MD[a,b], **Michael A. Turner, MD**[a,b], **Siamak Amirfakhri, PhD**[a,b], **Thinzar M. Lwin, MD**[c], **Mojgan Hosseini, MD**[d], **Pradipta Ghosh, MD**[e,f], **Marygorret Obonyo, PhD**[f], **Takashi Murakami, MD, PhD**[g], **Robert M. Hoffman, PhD**[a,b,h], **Paul J. Yazaki, PhD**[i], **Michael Bouvet, MD**[a,b,*]

[a]Department of Surgery, University of California San Diego, La Jolla, California

[b]Department of Surgery, VA San Diego Healthcare System, La Jolla, California

[c]Department of Surgical Oncology, City of Hope National Medical Center, Duarte, California

[d]Department of Pathology, University of California San Diego, La Jolla, California

[e]Department of Cellular and Molecular Medicine, University of California San Diego, La Jolla, California

[f]Department of Medicine, University of California San Diego, La Jolla, California

[g]Department of Microbiology, Saitama Medical University, Saitama, Japan

[h]AntiCancer Inc, San Diego, California

[i]Department of Immunology & Theranostics, Beckman Research Institute of the City of Hope, Duarte, California

Abstract

Introduction: Gastric cancer poses a major therapeutic challenge. Improved visualization of tumor margins at the time of gastrectomy with fluorescent tumor-specific antibodies could improve outcomes. The present report demonstrates the potential of targeting gastric cancer with a humanized anti-carcinoembryonic antigen (CEA) antibody in orthotopic mouse models.

Methods: MKN45 cells were injected subcutaneously into nude mice to establish xenograft models. Tumor fragments collected from subcutaneous models were then implanted into the

*Corresponding author. UCSD Moores UCSD Cancer Center, 3855 Health Sciences Drive #0987, La Jolla, CA 92093-0987. mbouvet@ucsd.edu (M. Bouvet).

Author Contributions

Kristin E. Cox wrote the manuscript and was actively involved in each step of the experimental process. Michael A. Turner, Siamak Amirfakhri, and Thinzar M. Lwin were involved in the experimental process and design. Mojgan Hosseini performed the pathologic evaluation of the gastric tumors. Pradipta Ghosh and Marygorret Obonyo edited the manuscript. Takashi Murakami established the MKN45-luc cell line and provided us with it for use. Robert M. Hoffman edited the manuscript. Paul J. Yazaki was involved in the experimental process and developed the humanized anti-CEA hT84.66-M5A antibody. Michael Bouvet was involved in the research design and all aspects of the experimental process.

Disclosure

RMH is a non-salaried affiliate of AntiCancer, Inc producing patient-derived orthotopic xenograft mouse models for contract research.

Meeting Presentation

Presented at The Academic Surgical Congress in Houston, Texas February 2023.

greater curvature of the stomach to establish orthotopic models. For tumor labeling, a humanized anti-CEA antibody (M5A) and IgG as a control, were conjugated with the near-infrared dye IRDye800CW. Time (24–72 h) and dose (50–100 mg) response curves were performed in subcutaneous models. Orthotopic models received 50 mg of M5A-IR800 or 50 mg IgG-IR800 as a control and were imaged after 72 h. Fluorescence imaging was performed on the mice using the LI-COR Pearl Imaging System.

Results: In subcutaneous models, tumor to background ratios (TBRs) reached 8.85 at 72 h. Median TBRs of orthotopic model primary tumors were 6.25 (interquartile range [IQR] 6.03–7.12) for M5A-IR800 compared to 0.42 (IQR 0.38–0.54) for control. Abdominal wall metastasis median TBRs were 13.52 (IQR 12.79–13.76) for M5A-IR800 and 3.19 (IQR 2.65–3.73) for the control. Immunohistochemistry confirmed CEA expression within tumors.

Conclusions: Humanized anti-CEA antibodies conjugated to near-infrared dyes provide specific labeling of gastric cancers in mouse models. Orthotopic models demonstrated bright and specific labeling with TBRs greater than ten times that of control. This tumorspecific fluorescent antibody is a promising potential clinical tool for improving visualization of gastric cancer margins at time of surgical resection.

Keywords

CEA; Gastric cancer; Orthotopic mouse model; Fluorescence; Fluorescent antibody; Tumor labeling

Introduction

Gastric cancer is the fifth most frequently diagnosed cancer and the third leading cause of cancer-related deaths world-wide.[1,2] The increased mortality compared to incidence is attributed to its advanced stage at the time of diagnosis. Currently, only complete surgical resection (R0) provides an opportunity for a cure. Unfortunately, while an R0 resection results in a 5-y survival of 60%, even a microscopic positive margin (R1 resection) results in a dramatic reduction in 5-y survival to 13.4%.[3] Imaging techniques that visualize tumor margins, nodal disease, and distant spread at the time of surgery could improve selection of patients that would benefit from gastrectomy and the subsequent rates of R0 resections.

Indocyanine green (ICG) with near-infrared (NIR) imaging has been used in gastric cancer surgery, though primarily for lymphadenectomy and visualization of vascular anatomy.[4] A 2001 study evaluating ICG for identification of sentinel lymph nodes found the sensitivity to be 90%.[5] In addition to identifying sentinel nodes, the use of ICG has been shown to increase the number of nodes collected during lymphadenectomy, especially in stations six through nine.[6] More recently, ICG has been used for identifying the primary tumor and assisting with surgical margins. Patients received submucosal injections of ICG into four quadrants of the tumor via endoscopy 1 d prior to surgery. Patients who received ICG had increased numbers of lymph nodes dissected, consistent with the literature. However, there was no difference observed in surgical margins between the groups (no positive margins and an average margin difference of 3 mm).[7]

While ICG has been shown to improve the number of lymph nodes collected, it is a nonspecific fluorescent dye. Targeted fluorescence with tumor-specific markers could improve visualization of tumor margins. The utility of antibodies conjugated to NIR fluorophores to brightly label pancreatic[8,9] and colorectal cancers[10–13] in mouse models has previously been well established. For gastric cancers, one potential target is carcinoembryonic antigen (CEA), an established tumor-associated marker for gastrointestinal tract malignancies.

Tissue overexpression of CEA was detected by immunohistochemistry in 90% of both intestinal and diffuse type gastric cancers, while carbohydrate antigen 19–9 was only expressed in 50% of gastric cancers.[14] Despite the high proportion of gastric cancers expressing CEA, serum levels have limited utility for screening or in the detection of recurrence. In a review on CEA expression by Shimada *et al.* that included 46 publications and over 8000 patients, the positive rates for serum CEA level at each stage of gastric cancer were as follows: stage I = 13.7 %, stage II = 23.0 %, stage III = 25.6 %, and stage IV = 39.5 %.[15]

Moriyama *et al.* evaluated the serum CEA levels of 790 patients who underwent R0 resection and found that of the 89 patients with recurrence, only 56% had elevated CEA levels.[16] While Shibata *et al.* found that 62% of patients (18 of 29) with recurrence never had an elevated serum CEA level.[17] Despite the low sensitivity of serum CEA levels, the high proportion of tumors expressing CEA make it an excellent marker for in-vivo fluorescence tumor labeling.

Although fluorescence labeling with anti-CEA antibodies has been extensively studied in pancreatic and colorectal cancers, there has been significantly less research on its application in gastric cancer.[18] Koga *et al.* reported on the use of Alexa Fluor 594 conjugated anti-CEA for labeling of MKN45, though background signals (signals from surrounding normal tissue) were high.[19] While bright labeling of tumor cells is important, a low background signal is crucial for a tumor markers' potential for future clinical use. The present study aimed to evaluate the ability of a humanized anti-CEA antibody (M5A) conjugated with a NIR 800 nm dye to target gastric cancer in orthotopic mouse models and achieve high tumor-to-background ratios.

Methods

Mouse models

All studies were approved by the San Diego Veterans Administration Medical Center Institutional Animal Care and Use Committee (IACUC) animal-use protocol A17–020 and UCSD IACUC protocol S99001. Athymic male and female nude mice, aged 4–6 wk were purchased from the Jackson Laboratory (Bar Harbor, ME). The animals were fed an autoclaved diet and housed in a barrier facility. Orthotopic mouse models were fed a chlorophyll-reduced diet for 2 wk prior to imaging (Envigo, Indianapolis, IN) to reduce autofluorescence. Prior to any surgical procedure, the mice were anesthetized with a solution of xylazine, ketamine, and phosphate-buffered saline (PBS) via intraperitoneal injection. For postoperative pain control, they received subcutaneous buprenorphine reconstituted in PBS

(dosage: 0.05 mg/kg). At the conclusion of the study, mice were anesthetized with isoflurane and euthanized by cervical dislocation.

Xenograft establishment

The gastric cancer cell line MKN45-luc (JCRB1370) was purchased from Sekisui XenoTech, LLC (Kansas City, MO). The cell line was established by Dr Takashi Murakami, Faculty of Medicine, Saitama Medical University, Saitama, Japan. Cells were cultured in Roswell Park Memorial Institute media with 10% fetal bovine serum and 1% penicillin. Subcutaneous models were established by injecting 1×10^6 cells in 100 μL per site into the bilateral flanks and shoulders of nude mice. Once subcutaneous tumors grew to approximately 1 cm, subsequent passages were performed by harvesting ~ 1 mm^3 fragments and implanting them in the bilateral flanks and shoulders of nude mice. Tumors were allowed to grow for ~ 4 wk prior to performing any imaging studies. In additional nude mice, orthotopic models were established using the method of surgical orthotopic implantation described by Furukawa *et al.*[20] In brief, mice were anesthetized as described above and a 1–2 cm transverse incision was made in the left upper quadrant through which the stomach was delivered. Subcutaneous-grown tumors were harvested and ~ 1 mm^3 fragments were affixed to the greater curve of the stomach using 8–0 nylon suture (Ethicon Inc, Somerville, NJ). The stomach was returned to the abdomen and the incision was closed with interrupted 6–0 vicryl sutures (Ethicon Inc.). Orthotopic models were allowed to grow for 4 wk prior to performing any imaging studies. An equal distribution of male and female mice was used for all experiments.

Antibody conjugation

The humanized anti-CEA hT84.66-M5A (M5A) monoclonal antibody, established by Yazaki *et al.*, was used for labeling of gastric cancer with immunoglobulin G (IgG) as a control.[21] Both M5A and IgG were conjugated to the NIR dye IRDye800CW (LI-COR Biosciences, Lincoln, NE) to establish M5A-IR800 and IgG-IR800 using methods previously described.[22,23] The final products were stored at 4°C.

Antibody-conjugate administration and imaging

M5A-IR800 antibody concentrations of 50 μg, 75 μg, or 100 μg were made by diluting the compound in PBS for a total injection volume of 100 μL. The antibodies were administered via tail vein injection to the subcutaneous tumor models (each dosage had a minimum of $n = 3$ for each timepoint) and imaged daily for 3 d using the Pearl Trilogy Small Animal Imaging System (LI-COR Biosciences) with 800 nm wavelength excitation. Orthotopic tumor models received 50 μg of M5A-IR800 ($n = 6$) or 50 μg of IgG-IR800 ($n = 5$) via tail vein injection. After 72 h, they were euthanized, and laparotomy was performed to allow imaging of intra-abdominal tissues.

Imaging and data processing

All images from the orthotopic models treated with either M5A-IR800 or IgG-IR800 were linked, and the same brightness and contrast settings were used across the images in the present study. Image studio, the proprietary imaging software for the Pearl Trilogy Small

Animal Imaging system was used for image analysis. Regions of interest (ROI) were marked around the tumors and background tissue using the bright light images. The system then quantified the mean fluorescence intensity of the 800 nm signal for each of these areas of interest. From this, TBRs were calculated. The following tissues were used as background for each experiment; skin for subcutaneous models, stomach for orthotopic models, and abdominal wall if an abdominal wall metastasis was present in the orthotopic model.

Immunohistochemistry

Tumor samples were removed en bloc with surrounding tissue at the time of mouse necropsy. Samples were fixed in formalin for at least 72 h prior to being embedded in paraffin and sectioned. Slides were stained with hematoxylin and eosin per standard protocols. Immunohistochemistry was performed per standard protocol using the humanized anti-CEA hT84.66-M5A antibody at a dilution of 1:1000 with secondary goat antihuman horseradish peroxidase (Southern Biotech Cat No. 2040–05) at a dilution of 1:200. Horseradish peroxidase was visualized by a diaminobenzidine chromogenic reaction. An experienced pathologist (M.H.) performed interpretation of the histologic slides.

Statistical analysis

Statistical analysis was performed using SPSS software (IBM, Armonk, NY). An analysis of variance was performed to compare the TBRs of the subcutaneous tumor models at varying dosages and timepoints. A Mann–Whitney *U* test with two tails was performed to compare the TBRs of M5A-IR800 *versus* IgG-IR800 in the orthotopic gastric cancer models, as the data did not meet criteria for normality. A *P* value of <0.05 was used as a predetermined cutoff for statistical significance.

Results

Targeting subcutaneous gastric cancer tumors

In subcutaneous models, time (24, 48, and 72 h) and dose-response (50 μg, 75 μg, or 100 μg) curves were established to identify the optimal M5A-IR800 administration to target MKN45 gastric cancer. Noninvasive imaging revealed highly specific tumor targeting and increasing TBRs over time (Fig. 1). When comparing TBRs at 24 h and 72 h, all treatment groups (50 μg, 75 μg, and 100 μg) showed a statistically significant difference between the two timepoints (with *P* values of 0.007, <0.001, and 0.046, respectively). At 72 h, the highest TBRs were seen for each dosage and ranged from 6.37 to 8.85. Given no statistically significant difference was observed between the treatment groups at 72 h, the lowest dose (50 μg) was selected for use in orthotopic models.

Bright labeling of orthotopic primary gastric tumors

Fluorescence imaging of orthotopic models revealed bright and specific labeling of gastric tumors with M5A-IR800 compared to control (Fig. 2A–B). At 72 h, a median TBR of 6.25 (interquartile range [IQR] 6.03–7.12) was seen in the M5A-IR800 group ($n = 6$) compared to 0.42 (IQR 0.38–0.54) for the control ($n = 5$) with a *P* value of 0.004 (Fig. 2C).

Labeling of metastases

M5A-IR800 brightly labeled a 2 × 4 mm intra-abdominal metastasis (Fig. 3A). Abdominal wall metastases were seen in a subset of the orthotopic models ($n = 2$ for each group). Bright and specific labeling was again seen with M5A-IR800 compared to control, and M5A-IR800 was able to label metastases as small as 2 mm (Fig. 3B–C). A median TBR of 13.52 (IQR 12.79–13.76) was seen with M5A-IR800 labeling of metastases compared to 3.19 (IQR 2.65–3.73) for the control (Fig. 3D).

Immunohistochemistry of orthotopic gastric cancer models

Hematoxylin and eosin staining of MKN45 orthotopic tumors showed poorly differentiated adenocarcinoma (Fig. 4A). CEA staining was strongly positive and confined to areas of adenocarcinoma (Fig. 4B), confirming the specific targeting of the M5A-IR800 antibody-dye conjugate.

Discussion

In the present study, we demonstrated that a humanized anti-CEA antibody (M5A) conjugated to a NIR dye could brightly and selectively label human gastric cancer in mouse models. Excellent TBRs were seen in both subcutaneous and orthotopic models with TBRs greater than 6 when imaged after 72 h. Additionally, robust labeling of intra-abdominal and abdominal wall metastases was observed. These findings show the potential CEA has for future clinical applications in targeted fluorescence guided surgery of gastric cancer.

The use of anti-CEA antibodies for detection of micrometastases has been previously explored in mouse models. Ito *et al.* demonstrated the ability of a NIR anti-CEA probe to detect peritoneal lesions as small as 1–2 mm compared to 6 mm for magnetic resonance imaging (MRI) using multiple human gastric cancer cell lines.[24] However, this study used cell injection into the peritoneal cavity as a peritoneal disease model and therefore, they are not true metastases. The present study used the technique of surgical orthotopic implantation described by Furukawa *et al.* as the metastatic pattern seen in orthotopic mouse models was found to correlate to the patients' pattern of disease from which the tumor samples were derived from.[20] Using this model, the present study demonstrates the detection of lesions as small as 2 mm by the M5A-IR800 probe.

A potential therapeutic use of anti-CEA was demonstrated by Shirasu *et al.* who performed photoimmunotherapy and showed an approximately two-thirds decrease in the rate of tumor growth 16 d after treatment in subcutaneous models of MKN45-luc.[25]

Advances in the clinical applications of CEA for multiple types of cancer are currently ongoing. One such clinical trial evaluated the use of anti-CEA antibodies to deliver Yttrium-90 DOTA to advanced solid tumors. Ten of the sixteen patients (all having previously progressed on standard therapy) had stable disease after 3 mo, while two patients had a greater than 50% reduction in serum CEA after the treatment. In an additional two patients, MRI following administration of this radiolabeled antibody revealed previously unknown brain metastases.[26]

The humanized anti-CEA antibody used in this present study, hT84.66-M5A, has successfully been used for positron emission tomography (PET) imaging when tagged with Copper-64 DOTA as described by Wong *et al.*[27] Twenty patients with a variety of CEA expressing cancers including colon, rectal, gastric, pancreatic, and medullary thyroid cancer were included. Four of eight patients with negative imaging were confirmed as true negatives. Ten of twelve patients with positive imaging had presence of disease confirmed by biopsy, surgery, or additional imaging. Of note, the computed tomography scan for one patient was initially read as negative, however, after the CEA scan showed evidence of disease, a second review of imaging revealed the presence of disease that was then confirmed with MRI.

Promising clinical use of anti-CEA (SGM-101) is currently ongoing for fluorescence-guided surgery of colorectal cancer using an IR700 dye. Phase I/II studies revealed tumor fluorescence in thirty out of thirty-seven patients with intraoperative TBRs of 1.5–2.4. Of the seven patients that were negative for fluorescence, all were found to have pathology confirmed complete response to neoadjuvant therapy.[28] A Phase III trial is currently actively recruiting (NCT03659448). Additionally, a similar Phase I clinical trial was conducted in twelve patients with pancreatic cancer using SGM-101.[29]

The data coming from these trials are encouraging for the future of fluorescence-guided surgery as well as the application of anti-CEA in other gastrointestinal cancers. To the best of our knowledge, the present study is the first to describe a tumor-specific imaging agent for orthotopic mouse models of gastric cancer. One limitation of this study, however, is the use of a single human cancer cell line which could theoretically produce a homogenous cell population. Future studies will include the use of patient-derived gastric cancers[30] to determine if anti-CEA M5A-IR800 will be widely applicable to primary and metastatic gastric cancers and to determine its potential to label lymph node metastases. Additional limitations include the depth of penetration of the fluorescence imaging which would lead to a decreased sensitivity for lesions that were not confined to the surface.[24] The use of NIR wavelength dyes (700–800 nm) have improved tissue depth penetration compared to visible wavelength dyes such as Alexa Fluor 488. However, in large organs such as the liver, depth of signal penetration is still a significant limitation.[31] This limitation could be addressed potentially using probes labeled with both an optical and radioactive imaging agent.[32,33]

Overall, NIR fluorescent anti-CEA antibodies are promising clinical tools for fluorescence-guided surgery which have the potential to improve outcomes of gastric cancer.

Funding

This work was supported by VA Merit Review (grant numbers 1 I01 BX003856-01A1 and 1 I01 BX004494-01), National Institute of Health (R01s CA256973-01, CA100768 and CA238042), Padres Pedal the Cause Collaborative Translational Pilot Project (#PTC2021 and #PCT2022), Department of Defense Award (W81XWH-20-1-0675), and National Institute of Health Training Grant (T32CA121938). The Tissue Technology Shared Resource is supported by a National Cancer Institute Cancer Center Support Grant (CCSG Grant P30CA23100). Other sources of support include the Torrey Coast Foundation.

REFERENCES

1. World Health Organization. International Agency for Research on Cancer. Globocan 2020: world fact sheet. 2020. Available at: https://gco.iarc.fr/today/data/factsheets/populations/900-world-fact-sheets.pdf. Accessed October 23, 2022.
2. Ajani JA, D'Amico TA, Bentrem DJ, et al. Gastric cancer, version 2.2022, NCCN clinical Practice guidelines in oncology. J Natl Compr Canc Netw. 2022;20:167–192. [PubMed: 35130500]
3. Wang SY, Yeh CN, Lee HL, et al. Clinical impact of positive surgical margin status on gastric cancer patients undergoing gastrectomy. Ann Surg Oncol. 2009;16:2738–22743. [PubMed: 19636636]
4. Belia F, Biondi A, Agnes A, et al. The use of indocyanine green (ICG) and near-infrared (NIR) fluorescence-guided imaging in gastric cancer surgery: a narrative review. Front Surg. 2022;9:880773. [PubMed: 35836598]
5. Hiratsuka M, Miyashiro I, Ishikawa O, et al. Application of sentinel node biopsy to gastric cancer surgery. Surgery. 2001;129:335–340. [PubMed: 11231462]
6. Kwon IG, Son T, Kim HI, Hyung WJ. Fluorescent lymphography-guided lymphadenectomy during robotic radical gastrectomy for gastric cancer. JAMA Surg. 2019;154:150–158. [PubMed: 30427990]
7. Liu M, Xing J, Xu K, et al. Application of near-infrared fluorescence imaging with indocyanine green in totally laparoscopic distal gastrectomy. J Gastric Cancer. 2020;20:290–299. [PubMed: 33024585]
8. Lwin TM, Murakami T, Miyake K, et al. Tumor-specific labeling of pancreatic cancer using a humanized anti-CEA antibody conjugated to a near-infrared fluorophore. Ann Surg Oncol. 2018;25:1079–1085. [PubMed: 29372363]
9. Turner MA, Hollandsworth HM, Nishino H, et al. Fluorescent anti-MUC5AC brightly targets pancreatic cancer in a patient-derived orthotopic xenograft. In Vivo. 2022;36:57–62. [PubMed: 34972700]
10. Hollandsworth HM, Lwin TM, Amirfakhri S, et al. Anti-Claudin-1 conjugated to a near-infrared fluorophore targets colon cancer in PDOX mouse models. J Surg Res. 2019;242:145–150. [PubMed: 31077946]
11. Hollandsworth HM, Amirfakhri S, Filemoni F, et al. Humanized anti-tumor-associated glycoprotein-72 for submillimeter near-infrared detection of colon cancer in metastatic mouse models. J Surg Res. 2020;252:16–21. [PubMed: 32217350]
12. Turner MA, Hollandsworth HM, Amirfakhri S, et al. Antimucin 4 fluorescent antibody brightly targets colon cancer in patient-derived orthotopic xenograft mouse models: a proof-of-concept study for future clinical applications. Am J Surg. 2022;224:1081–1085. [PubMed: 35715267]
13. Gutowski M, Framery B, Boonstra MC, et al. SGM-101: an innovative near-infrared dye-antibody conjugate that targetsCEA for fluorescence-guided surgery. Surg Oncol. 2017;26:153–162. [PubMed: 28577721]
14. Guazzi P, Zocco D, Isajevs S, et al. TM9SF4 expression in tumor tissues: a novel diagnostic biomarker for gastrointestinal tumors. Transl Cancer Res. 2020;9:6652–6659. [PubMed: 35117275]
15. Shimada H, Noie T, Ohashi M, Oba K, Takahashi Y. Clinical significance of serum tumor markers for gastric cancer: a systematic review of literature by the task force of the Japanese gastric cancer association. Gastric Cancer. 2014;17:26–33. [PubMed: 23572188]
16. Moriyama J, Oshima Y, Nanami T, et al. Prognostic impact of CEA/CA19–9 at the time of recurrence in patients with gastric cancer. Surg Today. 2021;51:1638–1648. [PubMed: 33682011]
17. Shibata C, Nakano T, Yasumoto A, et al. Comparison of CEA and CA19–9 as a predictive factor for recurrence after curative gastrectomy in gastric cancer. BMC Surg. 2022;22:213. [PubMed: 35655198]
18. Turner MA, Lwin TM, Amirfakhri S, et al. The use of fluorescent anti-CEA antibodies to label, resect and Treat cancers: a review. Biomolecules. 2021;11:1819. [PubMed: 34944463]
19. Koga S, Oshima Y, Honkura N, et al. In vivo subcellular imaging of tumors in mouse models using a fluorophore-conjugated anti-carcinoembryonic antigen antibody in two-photon excitation microscopy. Cancer Sci. 2014;105:1299–1306. [PubMed: 25117702]

20. Furukawa T, Fu X, Kubota T, Watanabe M, Kitajima M, Hoffman RM. Nude mouse metastatic models of human stomach cancer constructed using orthotopic implantation of histologically intact tissue. Cancer Res. 1993;53:1204–1208. [PubMed: 8439965]
21. Yazaki PJ, Sherman MA, Shively JE, et al. Humanization of the anti-CEA T84.66 antibody based on crystal structure data. Protein Eng Des Sel. 2004;17:481–489. [PubMed: 15316127]
22. DeLong JC, Murakami T, Yazaki PJ, Hoffman RM, Bouvet M. Near-infrared-conjugated humanized anti-carcinoembryonic antigen antibody targets colon cancer in an orthotopic nude-mouse model. J Surg Res. 2017;218:139–143. [PubMed: 28985840]
23. Hollandsworth HM, Nishino H, Turner M, et al. Humanized fluorescent tumor-associated glycoprotein-72 antibody selectively labels colon-cancer liver metastases in orthotopic mouse models. In Vivo. 2020;34:2303–2307. [PubMed: 32871754]
24. Ito A, Ito Y, Matsushima S, et al. New whole-body multimodality imaging of gastric cancer peritoneal metastasis combining fluorescence imaging with ICG-labeled antibody and MRI in mice. Gastric Cancer. 2014;17:497–507. [PubMed: 24288123]
25. Shirasu N, Yamada H, Shibaguchi H, Kuroki M, Kuroki M. Potent and specific antitumor effect of CEA-targeted photoimmunotherapy. Int J Cancer. 2014;135:2697–2710. [PubMed: 24740257]
26. Akhavan D, Yazaki P, Yamauchi D, et al. Phase I study of yttrium-90 radiolabeled M5A anti-carcinoembryonic antigen humanized antibody in patients with advanced carcinoembryonic antigen producing malignancies. Cancer Biother Radiopharm. 2020;35:10–15. [PubMed: 31910346]
27. Wong JYC, Yamauchi DM, Adhikarla V, et al. First-in-human Pilot PET immunoimaging study of 64Cu-Anti-carcinoembryonic antigen monoclonal antibody (hT84.66-M5A) in patients with carcinoembryonic antigen-producing cancers. Cancer Biother Radiopharm. 2023;38:26–37. [PubMed: 36154291]
28. de Valk KS, Deken MM, Schaap DP, et al. Dose-finding study of a CEA-targeting agent, SGM-101, for intraoperative fluorescence imaging of colorectal cancer. Ann Surg Oncol. 2021;28:1832–1844. [PubMed: 33034788]
29. Hoogstins CES, Boogerd LSF, Sibinga Mulder BG, et al. Image-guided surgery in patients with pancreatic cancer: first results of a clinical trial using SGM-101, a novel carcinoembryonic antigen-targeting, near-infrared fluorescent agent. Ann Surg Oncol. 2018;25:3350–3357. [PubMed: 30051369]
30. Furukawa T, Kubota T, Watanabe M, Kitajima M, Hoffman RM. Orthotopic transplantation of histologically intact clinical specimens of stomach cancer to nude mice: correlation of metastatic sites in mouse and individual patient donors. Int J Cancer. 1993;53:608–612. [PubMed: 8436434]
31. Maawy AA, Hiroshima Y, Kaushal S, Luiken GA, Hoffman RM, Bouvet M. Comparison of a chimeric anti-carcinoembryonic antigen antibody conjugated with visible or near-infrared fluorescent dyes for imaging pancreatic cancer in orthotopic nude mouse models. J Biomed Opt. 2013;18:126016. [PubMed: 24356647]
32. Lwin TM, Minnix M, Li L, et al. Multimodality PET and near-infrared fluorescence intraoperative imaging of CEA-positive colorectal cancer. Mol Imaging Biol. 2023;25:727–734. [PubMed: 37341873]
33. Hekman MC, Rijpkema M, Muselaers CH, et al. Tumor-targeted dual-modality imaging to improve intraoperative visualization of clear cell renal cell carcinoma: a first in man study. Theranostics. 2018;8:2161–2170. [PubMed: 29721070]

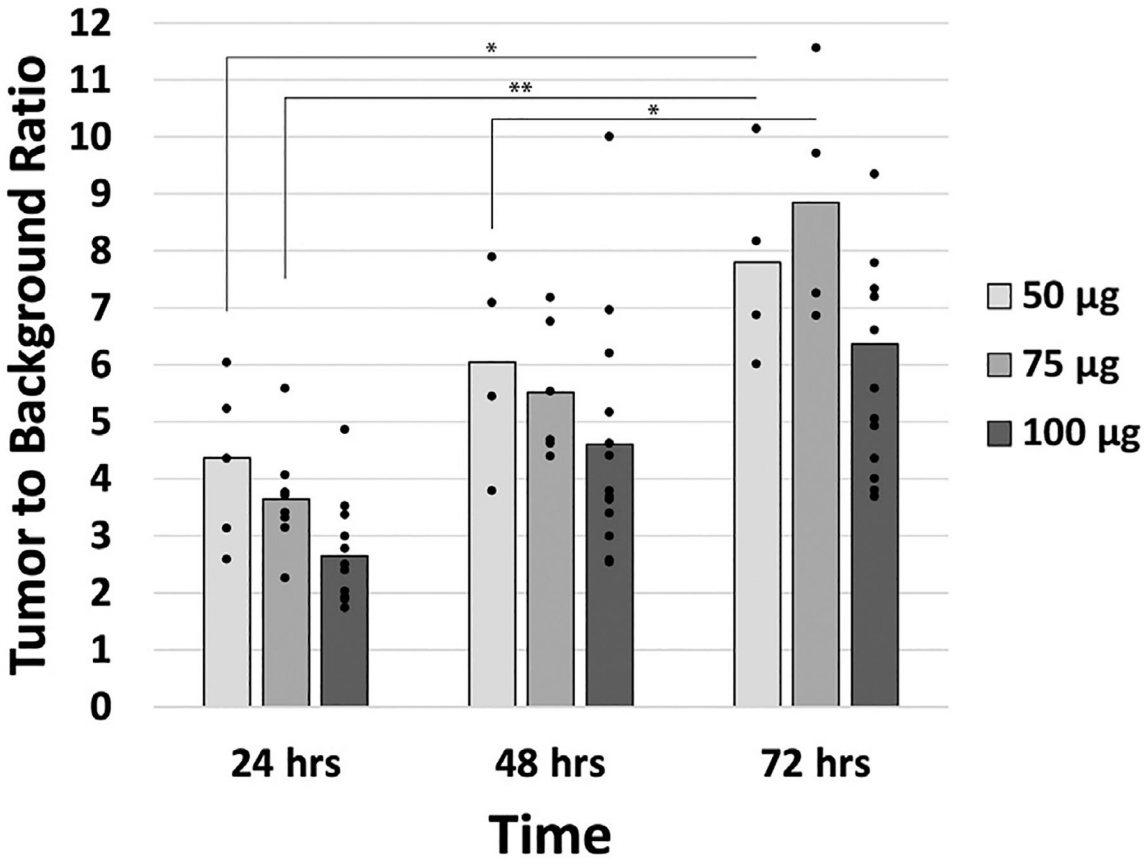

Fig. 1 –.

Tumor to background ratios (TBRs) in subcutaneous gastric cancer models. Mean TBRs of subcutaneous models of MKN45 labeled with M5A-IR800 at all doses (50 µg, 75 µg, or 100 µg) increased over time. Bar graphs represent mean and dots represent individual TBRs within the treatment group. * *P* value <0.05, ** *P* value <0.001.

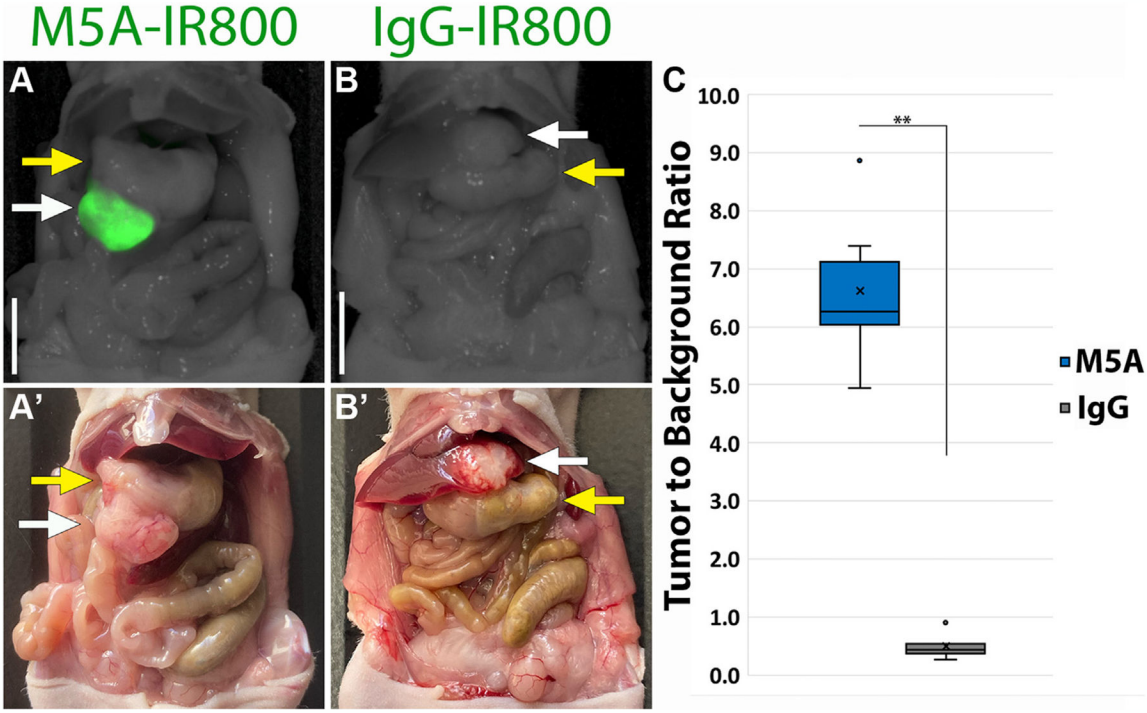

Fig.2 –.

Fluorescence labeling of orthotopic primary gastric tumors after 72 h. (A) M5A-IR800 50 μg brightly labels primary gastric tumor. (A') Bright light imaging of the gastric tumor growing from the greater curvature of stomach. (B) Lack of gastric tumor labeling with IgG-IR800 50 μg. (B') Bright light imaging of the gastric tumor shows it directly invading the liver parenchyma. White arrow: tumor, Yellow arrow: stomach. Scale bar: 1 cm. (C) Box and whisker plots of primary gastric tumor's tumor to background ratios (TBRs) labeled with M5A-IR800 or IgG-IR800. X: mean, line: median, dots: outliers. ** *P* value: 0.004.

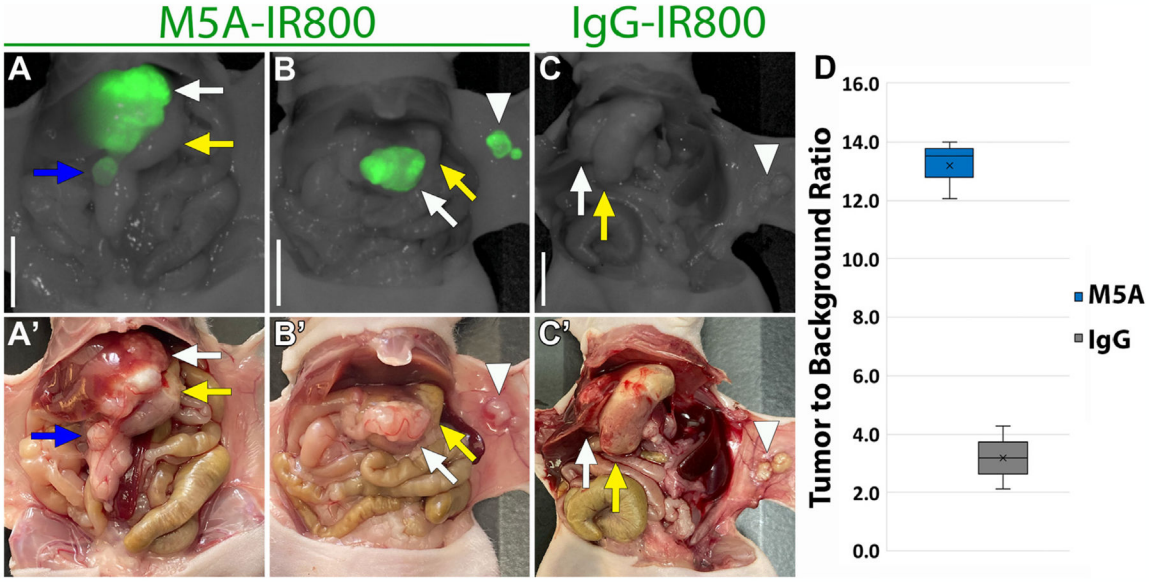

Fig. 3 –.

Fluorescence labeling of intra-abdominal and abdominal wall metastases after 72 h. (A) M5A-IR800 50 μg brightly labels a 2 × 4 mm intra-abdominal metastasis in addition to the primary tumor. (A') Bright light imaging of gastric tumor invading the liver parenchyma and an intra-abdominal metastasis. (B) M5A-IR800 50 μg brightly labels both the primary gastric tumor and abdominal wall metastases as small as 2 × 2 mm. (B') Bright light imaging with the gastric tumor seen on the greater curvature of stomach and two abdominal wall metastases. (C) IgG-IR800 50 μg does not label primary tumor nor abdominal wall metastases. (C') Bright light imaging with the gastric tumor seen directly invading the liver parenchyma and two small abdominal wall metastases. White arrow: tumor, yellow arrow: stomach, blue arrow: intra-abdominal metastasis, arrowhead: abdominal wall metastases. Scale bar: 1 cm. (D) Box and whisker plots of abdominal wall metastasis tumor to background ratios (TBRs) labeled with M5A-IR800 ($n = 2$) or IgG-IR800 ($n = 2$). ×: mean, line: median.

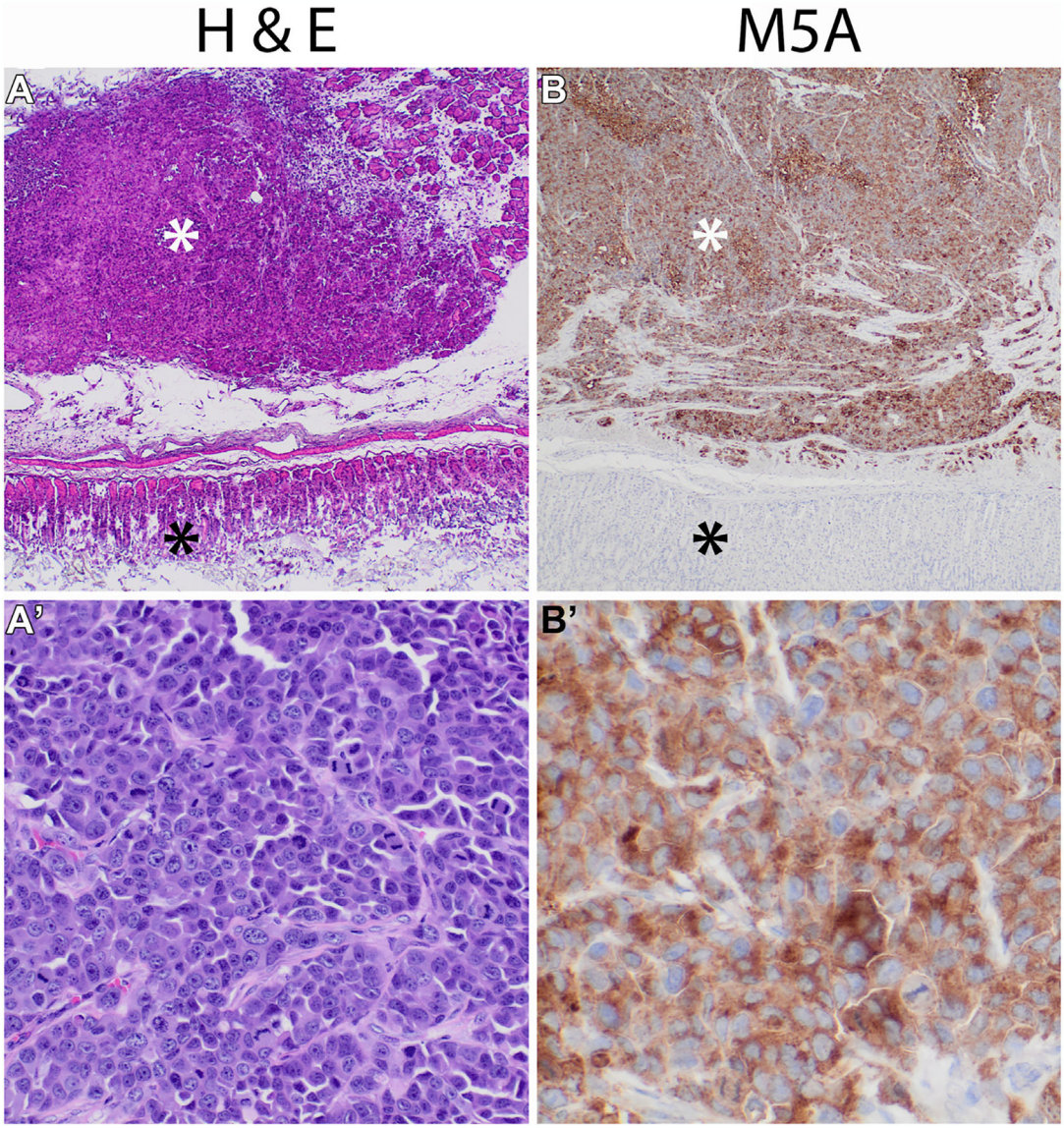

Fig. 4 –.

Carcinoembryonic antigen (CEA) expression of orthotopic gastric tumors. (A) hematoxylin and eosin (H&E) and (B) CEA staining at 4× magnification with tumor denoted by white asterisk, normal gastric tissue by black asterisk. (A') High power (20×) magnification of H&E staining showing poorly differentiated adenocarcinoma. (B') High power (40×) magnification with strong CEA staining of gastric adenocarcinoma.